



The Research on Composite Control Strategy of Active Power Filter

Chen Wenwen and Zhang Danhong

EasyChair preprints are intended for rapid dissemination of research results and are integrated with the rest of EasyChair.

April 20, 2019

The Research on Composite Control Strategy of Active Power Filter

Chen Wenwen, Zhang Danhong
School of automation
Wuhan University of Technology
Wuhan, China
cww19961114@whut.edu.cn

Abstract—In order to improve the performances of the active power filter used in a three-phase three-wire system, this paper proposes an integrated control system including the hysteresis controller and proportional resonance controller. The current loop controller and proportional integral voltage loop controller construct the proportional resonance controller. At first, the integrated control system measures the load harmonic current by the harmonic current detection algorithm. Then the proportional resonance controller and hysteresis controller generate the compensation current which has the same amplitude and reverses phase as the harmonic measurements. Finally, the compensation current is injected into the power grid to cancel the harmonic current. The simulation results show that the integrated control system tracks and compensates the harmonic current quickly, and it also mitigates the power system current distortion factor effectively.

Index Terms—Active power filter; Composite control strategy; Proportional resonance control; Harmonic compensation

I. INTRODUCTION

With the rapid development of the economy, the non-linear load is used more and more widely in the power grid, which greatly facilitates people's lives, but the harmonics generated during its use can cause the power quality of the grid to deteriorate[1, 2]. The reduction of power quality of the grid will affect the normal operation of the grid itself and reduce the reliability of the power equipment's operation. Therefore, how to control the harmonic pollution in the power grid is an important issue that needs to be dealt with urgently in the development of modern power. Currently, devices that suppress harmonics mainly include passive filters and active power filters. Passive power filters[3] are inexpensive, but it can only filter out pre-set frequency ranges and cannot change with load changes. At the same time, there will be serious consequences when the load fluctuates. Compared with passive power filters, active power filters[4, 5] (APFs) have the advantages such as high controllability, strong adaptive ability, fast response, small size, and lightweight. It is widely used to suppress harmonic devices. The key to APF control is the control of output current and DC side voltage[6]. The double closed cascade control of voltage outer loop and the current inner loop are common control strategy with simple structure and excellent control performance. In the double closed-loop control strategy, the main factor determining the

APF output accuracy is the current control strategy[7, 8], in which hysteresis control and PR control[9] are common control methods. The hysteresis controller[10, 11] has a simple structure and is easy to implement, but the hysteresis control has a large ripple and cannot eliminate the burrs existing in the grid current waveform. Proportional resonance (PR) control[12] can realize the harmonic tracking of harmonic signals, but the control parameter setting is cumbersome and the controller design is complicated.

Combined with the advantages of PR and hysteresis controllers, it is proposed that the lower harmonics are mainly hysteresis control, the higher harmonics are controlled by PR, and proportional integral (PI) is introduced to control the DC voltage. The system performance of APF is improved by a composite control strategy.

II. APF BASIC PRINCIPLES

According to the form of APF that is connected to the grid, it can be divided into the series APF and the parallel APF. The series APF is connected to the grid through a coupling transformer, which can be equivalent to a controlled voltage source, mainly to filter out voltage type harmonics and the effect of voltage fluctuations on the load. However, since the load current will flow through the series APF, the rated parameters of the transformer are larger, The volume, as well as the loss, are larger. In addition, the protection of the serial APF during normal operation, the switching at the start of work, and the exit after a failure are complicated. The parallel APF is connected to the power grid in parallel with the load through the reactor. It can be equivalent to a controlled current source, mainly to eliminate the influence of current type harmonics and current fluctuation on the load. Compared with the series APF, the parallel APF has the advantages of convenient switching, flexibility and simple protection, and is widely used in industrial practical applications. The principle of the parallel three-phase three-wire active power filter is shown in Figure 1.

In figure, U_{sa}, U_{sb}, U_{sc} is the three-phase grid voltage, i_{sa}, i_{sb}, i_{sc} is the three-phase grid current, V_{dc} is the DC side voltage, U_{ra}, U_{rb}, U_{rc} is the output voltage of the PWM converter, i_{La}, i_{Lb}, i_{Lc} is the load current, i_{ca}, i_{cb}, i_{cc} is the

compensation current, L and R is the equivalent resistance of the output inductor and switching losses.

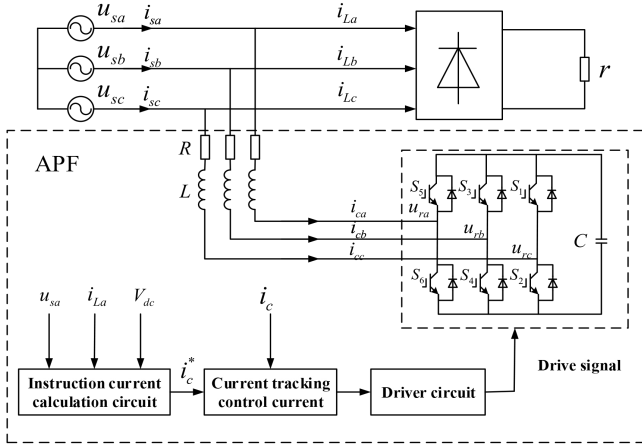


Fig. 1: Schematic diagram of the parallel APF system

Taking the single phase as an example, the basic principle of the parallel three-phase three-wire active power filter is explained. APF is a device[13] that compensates for distorted grid current. Thereby, it causes the grid current waveform to approximate or become a sine wave. It detects the three-phase power supply voltage and the current of non-linear load using the voltage and current sensor. The harmonic current detection algorithm is used to process the detected voltage and current signals to obtain the harmonic current to be compensated. A certain current control strategy[14] is used to track and control the switching state of the PWM converter in real time for the detected harmonic current so that the APF outputs and injects the actually required compensation current into the grid.

The principle of APF is briefly described as follows:

- (1) The grid current i_{sa} is equal to the sum of the load current i_{La} and the APF output current i_{ca} ;
- (2) The load current i_{La} is the sum of the load fundamental current i_{La1} and the load harmonic current i_{Lah} ;
- (3) When the APF output current i_{ca} is equal to the load harmonic current value i_{Lah} , the grid current i_{sa} is equal to the load fundamental current i_{La1} , which is a sine wave.

III. MAIN CIRCUIT DESIGN

The parallel type APF equivalent circuit is shown in Figure 2. The active power filter output compensation current meets:

$$L \frac{di_c(t)}{dt} + Ri_c(t) = u_c(t) - u_s(t) \quad (1)$$

Where $u_s(t)$ is the grid voltage, $u_c(t)$ is the AC voltage of the inverter in the APF, L is the filter inductor, and R is the equivalent resistance. In general, the R is small and therefore negligible. So the approximation is:

$$L \frac{di_c(t)}{dt} \approx u_c(t) - u_s(t) = \Delta u_{cs}(t) \quad (2)$$

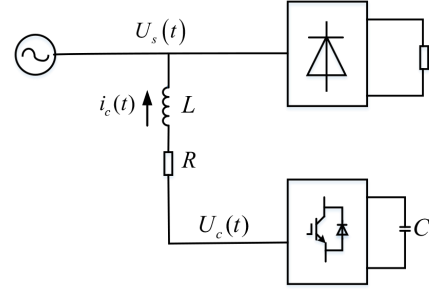


Fig. 2: Parallel APF equivalent circuit

As can be seen from the above formula, the magnitude of the AC side voltage $u_c(t)$ of the inverter determines the compensation current of the APF output. According to the modulation control principle of the voltage-type inverter, the voltage-type inverter can be equivalent to a proportional amplifier, namely:

$$u_c(t) = K_m V_{dc} \quad (3)$$

Where V_{dc} is the DC side voltage of the active power filter, and K_m is a function related to the modulation method. According to the above analysis, the main circuit parameters of the parallel APF include the selection of the DC side capacitor voltage, the selection of the DC side capacitor, and the design of the AC side filter inductor.

A. Filter inductor design

The compensation performance of the shunt active power filter mainly depends on whether the compensation current of the APF output can quickly and accurately track the harmonic current in the upper load current. The smaller the inductance L is, the stronger the current tracking capability of the APF is. At the same time, the suppression of the switching ripple current is weaker, which causes the current ripple of the APF output to be too large. When the active power filter fails, if the inductance L is too small, a large overcurrent will be generated, which will affect the system. Therefore, comprehensive considerations are needed. The empirical formula for estimating the inductance value is as follows:

$$L = \frac{4U_c t_c}{9\lambda i_{\max}^*} \quad (4)$$

Where λ is a constant, t_c is the control period, and i_{\max}^* is the maximum value of the compensation current.

The system parameters designed in this paper are as follows: $U_{dc} = 800V$, $T_s = 50\mu s$, $i_{\max}^* = 12A$, $\lambda = 0.5$, substituting the above formula can get 2.96mH, and the actual circuit selects the inductance value $L = 3mH$.

B. DC side capacitor voltage and capacitor design

The APF DC side voltage has a great influence on harmonic current compensation. To make the APF have better compensation effect, the DC side voltage needs to be kept constant. Therefore, the choice of DC side capacitor is very

important. The DC side capacitor of the active power filter is usually a large-capacity electrolytic capacitor. The selection of the capacitor is mainly determined by two parameters, one is the withstand voltage value of the capacitor, and the other is the capacitance capacity.

For a three-phase three-wire parallel APF, the DC-side voltage U_{dc} needs to be greater than twice the peak value of the grid phase voltage. The effective voltage of the phase voltage of the grid is $U = 200V$, and the phase voltage peak value is:

$$U_m = \sqrt{2}U = 311V \quad (5)$$

The DC side voltage U_{dc} should be greater than $2U_m$, so $U_{dc} > 622V$. Considering the grid voltage fluctuations and the filter inductance will produce a voltage drop, a certain margin must be left. The APF DC side voltage designed in this paper is set to 800V, that is $U_{dc} = 800V$. Therefore, the actual withstand voltage of the electrolytic capacitor needs to be greater than 800V.

For DC side voltage stability, the larger the DC side capacitor capacity, the more favorable the DC side voltage stability, but the large capacity capacitor will increase the cost and volume of the system. Therefore, the capacity of the DC side capacitor needs to be compromised. For a certain capacity APF, the DC side capacitance is determined by the DC side voltage, the APF capacity, and the DC side voltage fluctuation value. The specific calculation formula is as follows:

$$C_{dc} > \frac{P}{8f\varepsilon U_{dc}^2} \quad (6)$$

Where P is the compensation capacity of the APF, f is the grid frequency, and ε is the fluctuation amount. In this system, considering the cost and practical application, the DC side capacitor is selected to be $3300\mu F$.

IV. COMPOUND CONTROL STRATEGY

A. Harmonic current detection

The harmonic current detection algorithm is the core of harmonic control. The p-q harmonic current detection method based on the three-phase instantaneous reactive power theory is improved to obtain the $i_p - i_q$ method. Because it does not need to detect the three-phase grid voltage, the $i_p - i_q$ method has more accurate operation results in the case of grid waveform distortion.

When the three-phase power supply voltage is sinusoidally symmetrical, the relationship is listed as follows:

$$p = ei_p \quad (7)$$

$$q = ei_q \quad (8)$$

$$\begin{aligned} \begin{bmatrix} p \\ q \end{bmatrix} &= \begin{bmatrix} e_\alpha & e_\beta \\ e_\beta & -e_\alpha \end{bmatrix} \begin{bmatrix} i_\alpha \\ i_\beta \end{bmatrix} \\ &= \sqrt{\frac{3}{2}}E_m \begin{bmatrix} \sin \omega t & -\cos \omega t \\ -\cos \omega t & -\sin \omega t \end{bmatrix} \begin{bmatrix} i_\alpha \\ i_\beta \end{bmatrix} \end{aligned} \quad (9)$$

Substituting equation (7),(8) into equation (9), the formula is listed as follows:

$$\begin{aligned} \begin{bmatrix} i_p \\ i_q \end{bmatrix} &= \sqrt{\frac{3}{2}} \begin{bmatrix} \sin \omega t & -\cos \omega t \\ -\cos \omega t & -\sin \omega t \end{bmatrix} \\ &* \begin{bmatrix} 1 & -\frac{1}{2} & -\frac{1}{2} \\ 0 & \frac{\sqrt{3}}{2} & -\frac{\sqrt{3}}{2} \end{bmatrix} \begin{bmatrix} i_b \\ i_b \\ i_c \end{bmatrix} \end{aligned} \quad (10)$$

Considering that the three-phase current is non-sinusoidal, the three-phase current is subjected to fourier decomposition.

$$\begin{cases} i_a = \sum_{k=t}^{\infty} I_{km} \sin(k\omega t - \theta_k) \\ i_b = \sum_{k=1}^{\infty} I_{km} \sin[k(\omega t - \frac{2\pi}{3}) - \theta_k] \\ i_c = \sum_{k=t}^{\infty} I_{km} \sin[k(\omega t + \frac{2\pi}{3}) - \theta_k] \end{cases} \quad (11)$$

Where $k = 1, 3, 5, \dots$

Substitute equation (11) into equation (10) yields:

$$\begin{bmatrix} i_p \\ i_q \end{bmatrix} = \sqrt{\frac{3}{2}} \sum_{k=1}^{\infty} I_{km} \begin{bmatrix} \pm \cos[(k \mp 1)\omega t - \theta_k] \\ -\sin[(k \mp 1)\omega t - \theta_k] \end{bmatrix} \quad (12)$$

For the three-phase three-wire system expression, $k = 3, 6, 9, \dots$ component is not included. When $k = 1$, the i_p and i_q components reflect the fundamental component of the three-phase current, which is defined as i_{p1} and i_{q1} . When $k \neq 1$, the i_p and i_q components reflect the fundamental component of the three-phase current, which is defined as i_{ph} and i_{qh} .

$$\begin{bmatrix} i_p \\ i_q \end{bmatrix} = \begin{bmatrix} i_{p1} \\ i_{q1} \end{bmatrix} + \begin{bmatrix} i_{ph} \\ i_{qh} \end{bmatrix} \quad (13)$$

$$\begin{bmatrix} i_{p1} \\ i_{q1} \end{bmatrix} = \sqrt{\frac{3}{2}} I_{1m} \begin{bmatrix} \cos \theta_1 \\ \sin \theta_1 \end{bmatrix} \quad (14)$$

$$\begin{bmatrix} i_{ph} \\ i_{qh} \end{bmatrix} = \sqrt{\frac{3}{2}} \sum_{k=5}^{\infty} I_{km} \begin{bmatrix} \pm \cos(k \mp 1)\omega t - \theta_k \\ -\sin(k \mp 1)\omega t - \theta_k \end{bmatrix} \quad (15)$$

It can be seen from the above equation that after the three-phase current is transformed, i_{p1} and i_{q1} corresponding to the fundamental component becomes a direct current component, while i_{ph} and i_{qh} ($k = 6m \mp 1, m = 1, 2, 3, \dots$) corresponding to the higher harmonic component is converted into $6m$ harmonic components. To obtain the fundamental component of the transformed current, it is only necessary to use a low-pass filter to filter out the DC component \bar{i}_p and \bar{i}_q from the transformed current i_p and i_q . The schematic diagram is shown in Figure 3.

In Figure 3, the transformation formula is listed as follows:

$$C_{32} = \sqrt{\frac{2}{3}} \begin{bmatrix} 1 & -\frac{1}{2} & -\frac{1}{2} \\ 0 & \frac{\sqrt{3}}{2} & -\frac{\sqrt{3}}{2} \end{bmatrix} \quad (16)$$

$$C = \begin{bmatrix} \sin \omega t & -\cos \omega t \\ -\cos \omega t & \sin \omega t \end{bmatrix} \quad (17)$$

$$C_{23} = C_{32}^T \quad (18)$$

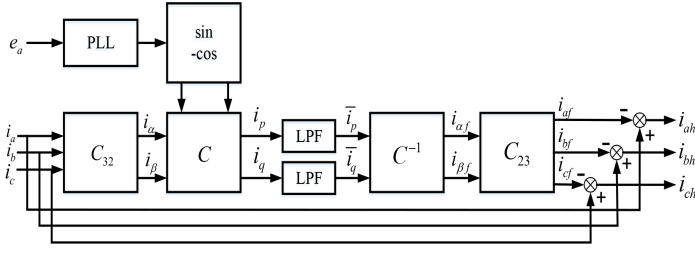


Fig. 3: Schematic diagram of detection method

The load three-phase current i_{La}, i_{Lb}, i_{Lc} is C_{32} transformed and C transformed to obtain the instantaneous active current and instantaneous reactive current in the d-q coordinate system. The high-frequency signal is filtered by a low-pass filter (LPF) to obtain a DC component and finally obtained by C^{-1} transformation and C_{23} transformation. The fundamental current in the a-b-c coordinate system. The load current is subtracted from the fundamental current to obtain the harmonic current i_{ca}, i_{cb}, i_{cc} that needs to be compensated.

B. Current Control Strategy

The current loop control strategy in this paper combines the proportional resonance control (PR) with the hysteresis comparator. In the case of low-order harmonics, the hysteresis comparator acts as the primary control and rapidly reduces the error. In the case of higher harmonics, the PR controller plays a major control role and improves control accuracy. The APF current loop control block diagram is shown in Figure 4.

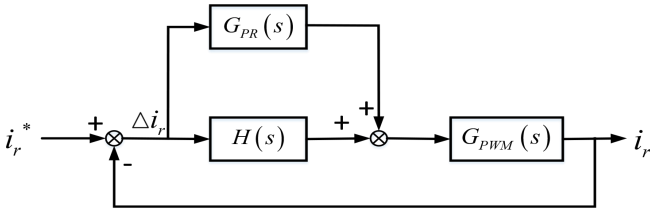


Fig. 4: Current loop control

In Figure , i_r is the PWM inverter output compensation current, and i_r^* is the compensation command signal.

The hysteresis comparator has two states according to the system error magnitude. The specific structure is shown in Figure 5.

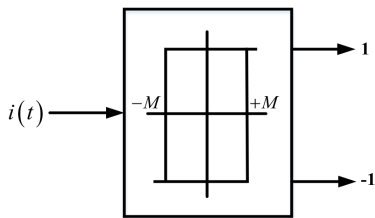


Fig. 5: Hysteresis-loop structure

$$H(t) = \begin{cases} 1 & D\Delta i_r > +M \\ -1 & D\Delta i_r < -M \end{cases} \quad (19)$$

Where M is the error threshold determined by the actual system, and Δi_r is the deviation between the PWM inverter output compensation current and the command signal.

The PR controller is suitable for the DC circuit voltage control system in APF. It not only has better stability in the frequency domain but also has better compensation effect for higher harmonics. The transfer function is as follows:

$$G_{PR}(s) = K_P + \frac{2K_{rm}\omega_c s}{s^2 + 2\omega_c s + (m\omega_s)^2} \quad (20)$$

Where K_P is the proportional coefficient, K_{rm} is the resonance coefficient at the m th harmonic ω_c is the cutoff frequency, ω_s is the resonant frequency.

The PWM inverter transfer function is:

$$G_{PWM}(s) = \frac{K_{PWM}}{T_{PWM}s + 1} \quad (21)$$

Where K_{PWM} is the equivalent magnification of the inverter, T_{PWM} is the control time constant of the system.

The output compensation current is:

$$i_r(s) = \frac{[G_{PR}(s) + H(s)]G_{PWM}(s)}{1 + [G_{PR}(s) + H(s)]G_{PWM}(s)} i_r^*(s) \quad (22)$$

Where $i_r(s)$ is the Laplace transform of the output compensation current function $i_r(t)$, $i_r^*(s)$ is the Laplace transform of the compensation current function $i_r^*(t)$, and $H(s)$ is the Laplace transform of the hysteresis function.

The open loop transfer function of the current loop is listed as follows:

$$M(s) = [G(s)H(s)]G_{PWM}(s) \quad (23)$$

C. Voltage control strategy

When performing compensation, the ACF device's own DC capacitor voltage must be stable[15]. Otherwise, it will affect the compensation effect. Second, the actual withstand voltage of the capacitor and IGBT is limited. If the voltage is uncontrollable, it will result in safety problems. Therefore, the voltage regulation strategy is very important. APF not only guarantees the accuracy of the compensation current but also the stability of the bus voltage on the DC side. Therefore, the PI control link is introduced on the DC side. The control block diagram is shown in Figure 6.

The difference Δu_{dc} between the detected DC side voltage actual value u_{dc} and the reference value u_{dc}^* is the PI controller input signal. And the PI adjustment controller is output as a superposition of the fundamental effective current adjustment amount \bar{i}_p and the effective DC component Δi_p of the harmonic command current. The three-phase fundamental current is obtained by C^{-1} transformation and C_{23} transformation, thereby obtaining a command compensation current after PI control.

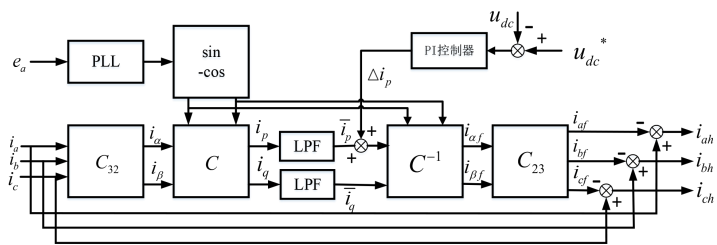


Fig. 6: DC side voltage PI control block diagram

V. SIMULATION

The simulation circuit is built in Simulink. The grid phase voltage is 220V and the frequency is 50Hz. The non-linear load is a three-phase rectifier bridge with inductive load. The resistance is 20Ω , the inductance is 3mH, the DC side voltage reference value is 800V, and the DC side capacitor is $3000\mu F$. Set the sampling time to $50 \times 10^{-6}s$.

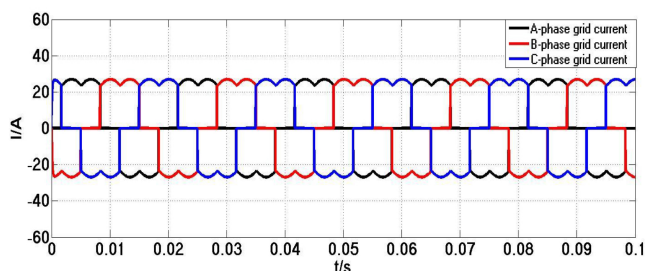


Fig. 7: The grid circuit waveform without the active power filter

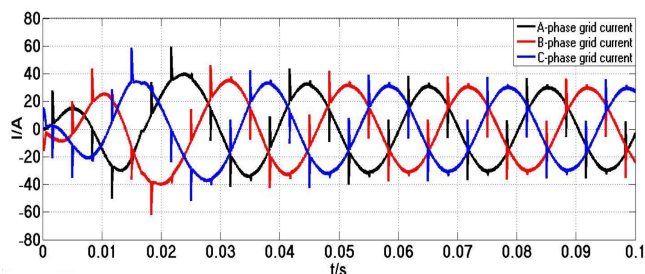


Fig. 8: The grid current waveform under the hysteresis comparison control

The grid circuit waveform without active power filter is shown in Figure 7. The grid current waveform and its spectrum analysis under the traditional hysteresis comparison control are shown in Figures 8 and 9. The grid current waveform, spectrum analysis and DC side voltage waveforms using the PR and hysteresis comparators are shown in Figures 10, 11 and 12. Comparing Fig. 8 and Fig. 10, the grid current under the traditional grid hysteresis control is significantly compensated, but the burrs are more, while the waveform the PR and the hysteresis comparator combined control is smoother. Comparing Fig. 9 with Fig. 11, the harmonic distortion rate is

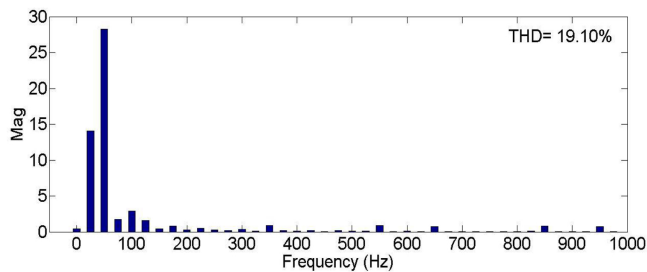


Fig. 9: FFT analysis under the hysteresis comparison control

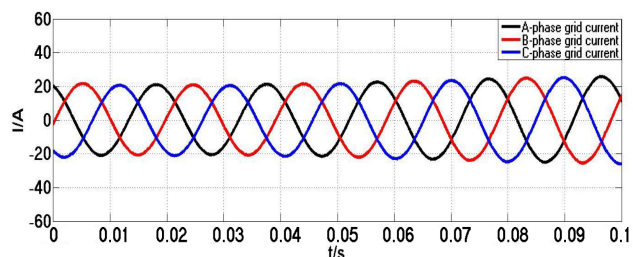


Fig. 10: The grid current waveform under the PR and the hysteresis comparator combined control

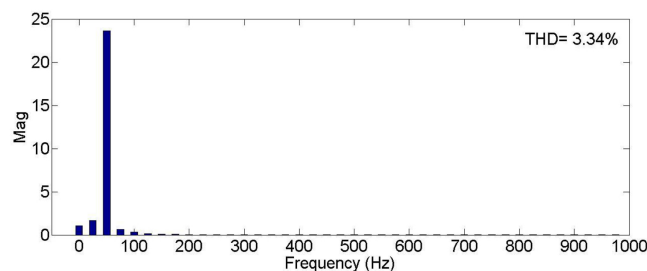


Fig. 11: FFT analysis under the PR and the hysteresis comparator combined control

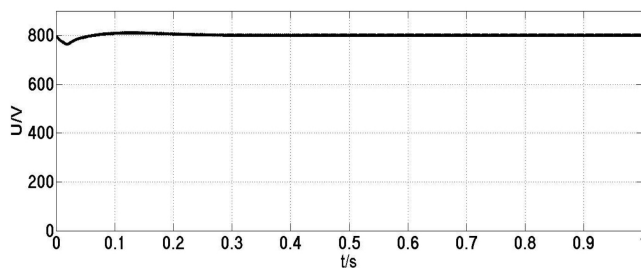


Fig. 12: DC side voltage waveform

significantly reduced under the combined control of PR and hysteresis comparator. It can be seen from Fig. 12 that the DC side voltage tends to be stabilized by PI control. The simulation results indicate that the APF under the control of the composite control strategy can better track and compensate the harmonic current and less waveform glitch, which verifies the effectiveness of the control strate.

VI. CONCLUSION

This paper first analyzes the basic principle of APF, then designs the main circuit parameters, and finally proposes a composite control strategy. The current loop is based on reactive power harmonic detection method, combined with PR control and hysteresis control to track and compensate harmonics. The voltage loop uses a more common PI control strategy. Through simulation modeling on Simulink, the simulation results show that the composite control strategy can effectively reduce the harmonic distortion rate under the condition that the parameter setting meets the requirements, and has high real-time and compensation accuracy.

REFERENCES

- [1] Xie C, Zhao X, Savaghebi M, et al. Multirate Fractional-Order Repetitive Control of Shunt Active Power Filter Suitable for Microgrid Applications[J]. *IEEE Journal of Emerging and Selected Topics in Power Electronics*. 2017, 5(2): 809-819.
- [2] P. T, N. Y. Design of current source hybrid power filter for harmonic current compensation[J]. *Simulation Modelling Practice and Theory*. 2015, 52: 78-91.
- [3] Song Y, Wang J, Monti A. Design of systematic parameter tuning approaches for multiple proportional-resonance AC current regulator[C]. *IEEE*, 2015.
- [4] Jiang W, Ding X, Ni Y, et al. An Improved Deadbeat Control for a Three-Phase Three-Line Active Power Filter With Current-Tracking Error Compensation[J]. *IEEE Transactions on Power Electronics*. 2018, 33(3): 2061-2072.
- [5] Zou Z, Zhou K, Wang Z, et al. Frequency-Adaptive Fractional-Order Repetitive Control of Shunt Active Power Filters[J]. *IEEE Transactions on Industrial Electronics*. 2015, 62(3): 1659-1668.
- [6] Briz F, Garcia P, Degner M W, et al. Dynamic Behavior of Current Controllers for Selective Harmonic Compensation in Three-Phase Active Power Filters[J]. *IEEE Transactions on Industry Applications*. 2013, 49(3): 1411-1420.
- [7] Mannen T, Fukasawa I, Fujita H. A New Control Method of Suppressing DC Capacitor Voltage Ripples Caused by Third-Order Harmonic Compensation in Three-Phase Active Power Filters[J]. *IEEE Transactions on Industry Applications*. 2018, 54(6): 6149-6158.
- [8] Shu Z, Liu M, Zhao L, et al. Predictive Harmonic Control and Its Optimal Digital Implementation for MMC-Based Active Power Filter[J]. *IEEE Transactions on Industrial Electronics*. 2014.
- [9] Hongda Cai W W Y P. Fuzzy Proportional-Resonant Control Strategy for Three-Phase Inverters in Islanded Micro-Grid with Nonlinear Loads[J]. 2014.
- [10] Nie C, Wang Y, Lei W, et al. An Enhanced Control Strategy for Multiparalleled Grid-Connected Single-Phase Converters With Load Harmonic Current Compensation Capability[J]. *IEEE Transactions on Industrial Electronics*. 2018, 65(7): 5623-5633.
- [11] Luo A, Shuai Z, Zhu W, et al. Development of Hybrid Active Power Filter Based on the Adaptive Fuzzy Dividing Frequency-Control Method[J]. *IEEE Transactions on Power Delivery*. 2009, 24(1): 424-432.
- [12] Lam C, Choi W, Wong M, et al. Adaptive DC-Link Voltage-Controlled Hybrid Active Power Filters for Reactive Power Compensation[J]. *IEEE Transactions on Power Electronics*. 2012, 27(4): 1758-1772.
- [13] Luo A, Xu X, Fang L, et al. Feedback-Feedforward PI-Type Iterative Learning Control Strategy for Hybrid Active Power Filter With Injection Circuit[J]. *IEEE Transactions on Industrial Electronics*. 2010, 57(11): 3767-3779.
- [14] Zhang H, Da Sun C, Li Z, et al. Voltage Vector Error Fault Diagnosis for Open-Circuit Faults of Three-Phase Four-Wire Active Power Filters[J]. *IEEE Transactions on Power Electronics*. 2017, 32(3): 2215-2226.
- [15] Dang P, Ellinger T, Petzoldt J. Dynamic Interaction Analysis of APF Systems[J]. *IEEE Transactions on Industrial Electronics*. 2014, 61(9): 4467-4473.